
STRENGTH
AND PLASTICITY

Resistance of Laser-Clad Chromium–Nickel Coatings to Failure under Contact Fatigue Loading

R. A. Savrai*

Institute of Engineering Science, Ural Branch, Russian Academy of Sciences, Ekaterinburg, 620049 Russia

**e-mail: ras@imach.uran.ru*

Received January 21, 2018; in final form, April 17, 2018

Abstract—This paper presents the results of our study of the contact endurance of laser-clad chromium–nickel coatings of the NiCrBSi system with different contents of chromium, boron, and carbon (PG-SR2, containing 0.48% C, 14.8% Cr, 2.1% B wt %; and PG-10N-01, containing 0.92% C, 18.2% Cr, 3.3% B wt %) and with additions of carbides of titanium TiC (15 and 25 wt %) and chromium Cr₃C₂ (15 wt %) upon contact fatigue loading according to the scheme of the pulsing non-impact “sphere-to-surface” contact. It has been established that the contact endurance of chromium–nickel coatings with different chemical compositions and different dispersity of structure is determined by their ability to resist plastic deformation under the conditions of repeated elastic–plastic deformation upon the mechanical non-impact contact action. This study has shown that composite coatings can be created, which contain large (50–150 μm) particles of the strengthening phases, whose contact endurance will not be substantially inferior to the contact endurance of coatings with fine (1–10 μm) strengthening phases. An estimation of the ability of the surface of the coatings to resist the mechanical contact action was made with the use of the data on microindentation. It has been shown that the method of microindentation (single loading) can be used for determining the ability of chromium–nickel coatings to withstand repeated contact loadings.

Keywords: laser cladding, chromium–nickel coatings, structure, phase composition, microindentation, contact fatigue

DOI: 10.1134/S0031918X18100113

INTRODUCTION

The application of coatings using the method of gas powder laser cladding, when a thin surface layer of the base metal is melted by a laser beam together with an added material [1], is an efficient method of strengthening as it increases wear resistance and restores the worn surfaces of machine parts. Coatings on the chromium–nickel basis, particularly the alloys of the NiCrBSi system [2–4], are applied widely, which, together with outstanding technological properties [5], have good characteristics of wear resistance, corrosion resistance, and thermal stability [2, 6–13].

We already know that one of the reserves for a further increase in the wear resistance of NiCrBSi coatings is the creation of composite coatings on their basis by the introduction into the composition of the powders of different additives, for example, TiC, WC, Cr₃C₂, SiC, TaC, Al₂O₃, Fe₂O₃, V₂O₅. The use of titanium carbide TiC in particular, which has high values of hardness, modulus of elasticity, and melting point, and also high thermal and chemical stability [7, 14–16], makes it possible to produce NiCrBSi–TiC composite coatings with increased hardness and wear resistance [13, 17, 18].

Along with the important characteristic of wear resistance, which determines the quality of many engineering materials and coatings, the ability of a material to sustain contact loads is also important [19], and this is usually evaluated according to the character of the fracture after single or repeated (cyclic) loading of the surface by the indenters of various shapes [19–28]. A single loading does not always make it possible to adequately estimate the resistance of the material to external contact actions because it does not take processes of fatigue degradation [21, 22] into account. Furthermore, additives of various strengthening particles can have different effects on the durability of coatings under the conditions of mechanical contact action. Therefore, it is important to perform an analysis of the contact endurance of coatings.

Instrumented microindentation has been used more often in recent years to study the micromechanical characteristics of chromium–nickel coatings, which, on the basis of the continuous registration of the diagram of loading–unloading in the “load–indenter-displacement” coordinates allows us to determine different characteristics of a material, including its strength properties [29, 30]. The use of a method of microindentation for evaluating the resis-

Table 1. Chemical composition of the coatings

Powder grade	Content of elements, wt %					
	C	Cr	Ni	Fe	Si	B
PG-SR2	0.48	14.8	Base	2.6	2.9	2.1
PG-10N-01	0.92	18.2	Base	3.4	4.2	3.3

tance to different mechanisms of wear and, correspondingly, wear resistance of steels of different classes [31, 32], and chromium–nickel [4, 33] and boride [34, 35] coatings was substantiated. It is of interest to us to use this method for evaluating the ability of the surface of chromium–nickel coatings to resist mechanical contact actions.

This work was aimed at investigating the contact endurance of laser-clad chromium–nickel coatings of the NiCrBSi system with different contents of chromium, boron, and carbon, and with additions of carbides of titanium TiC and chromium Cr₃C₂ upon the contact fatigue loading, and also allowed us the opportunity to use the method of instrumented microindentation for determining the ability of coatings with a structure of different dispersity to sustain the repeated contact loadings.

EXPERIMENTAL

We used the powders of grades PG-SR2 and PG-10N-01 (chromium–nickel alloys of the NiCrBSi system) of the granulometric composition of 40–160 μm as the materials for creating coatings (Table 1). For creating composite coatings with the additions of titanium carbide, we employed a powder mixture obtained by mixing the powders of grades PG-SR2 and of titanium carbide TiC of the granulometric composition of 50–150 μm in quantities of 15 and 25 wt %. For creating the composite coating with the addition of the chromium carbide, the powder mixture obtained by mixing the powders of grades PG-SR2 and 15 wt % chromium carbide Cr₃C₂ of the granulometric composition of 50–150 μm was taken.

We carried out the cladding of powders to the plates made of steel of St3 using a continuously operating CO₂ laser with a radiation power of 1.4–1.6 kW, a travelling speed of 160–200 mm/min, a flow rate of pow-

der 2.9–4.9 g/min, and the size of the laser spot on the surface of 6 × 1.5 mm. We transported the powder mixture into the zone of cladding by an inert gas (argon) at a pressure of 0.5 atm. To decrease surface stresses, we performed the cladding in two steps by overlaying one layer on the other [27]. After the cladding, the coatings were mechanically grinded to a thickness of 0.8–1.2 mm to eliminate surface waviness.

We conducted the mechanical tests for contact fatigue using an Instron 8801 servohydraulic installation equipped with a special mounting of original construction [36] according to a scheme of pulsing non-impact “sphere-to-surface” contact (Fig. 1) at a load cyclically changing according to a periodic (sinusoidal) law; the diameter of the steel sphere was 12.7 mm; the initial load $P_0 = 0.1$ kN; the peak load $P_{\max} = 8.7$ kN; the frequency of the loading pulses $f = 35$ Hz; the number of loading cycles $N = 10^6$. For the contact–fatigue tests, rectangular samples were used prepared from the clad plates with a size of 85 × 10 × 5 mm. At a given number of loading cycles, we carried out no fewer than two tests.

We studied the structure of coatings using a Tescan VEGA II XMU scanning electron microscope. We determined the microhardness using the method of the restored imprint using Leica VMHT, Wilson & Wolpert 402 MVD and Shimadzu HVM-G21DT microhardness-meter devices at a load of 0.98 N, speed of loading 40 m/s, and a holding under the load for 15 s.

We conducted instrumented microindentation with the recording of the diagram of loading using a Fischerscope HM2000 XYm measuring system with a Vickers indenter and a WIN-HCU software at a peak load of 1.98 N, time of loading of 5 s, holding under a load for 20 s, and the time of unloading of 5 s. The maximum indentation depth h_{\max} and the permanent indentation depth after the removal of the load h_p , the contact modulus of elasticity E^* ($E^* = E(1 - \nu^2)$, where E is the Young’s modulus, and ν is the Poisson’s ratio), the indentation hardness at the peak load H_{IT} , the Martens hardness HM, the elastic reverse deformation work of the indentation W_e , and the total mechanical work of the indentation W_t were determined according to the International Standard ISO 14577 [37]. The error of measurements of the microhardness and of the characteristics of the instrumented indentation was determined with a confidence coefficient $p = 0.95$.

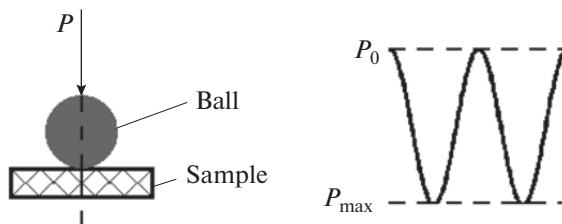


Fig. 1. Scheme of mechanical tests for contact fatigue.

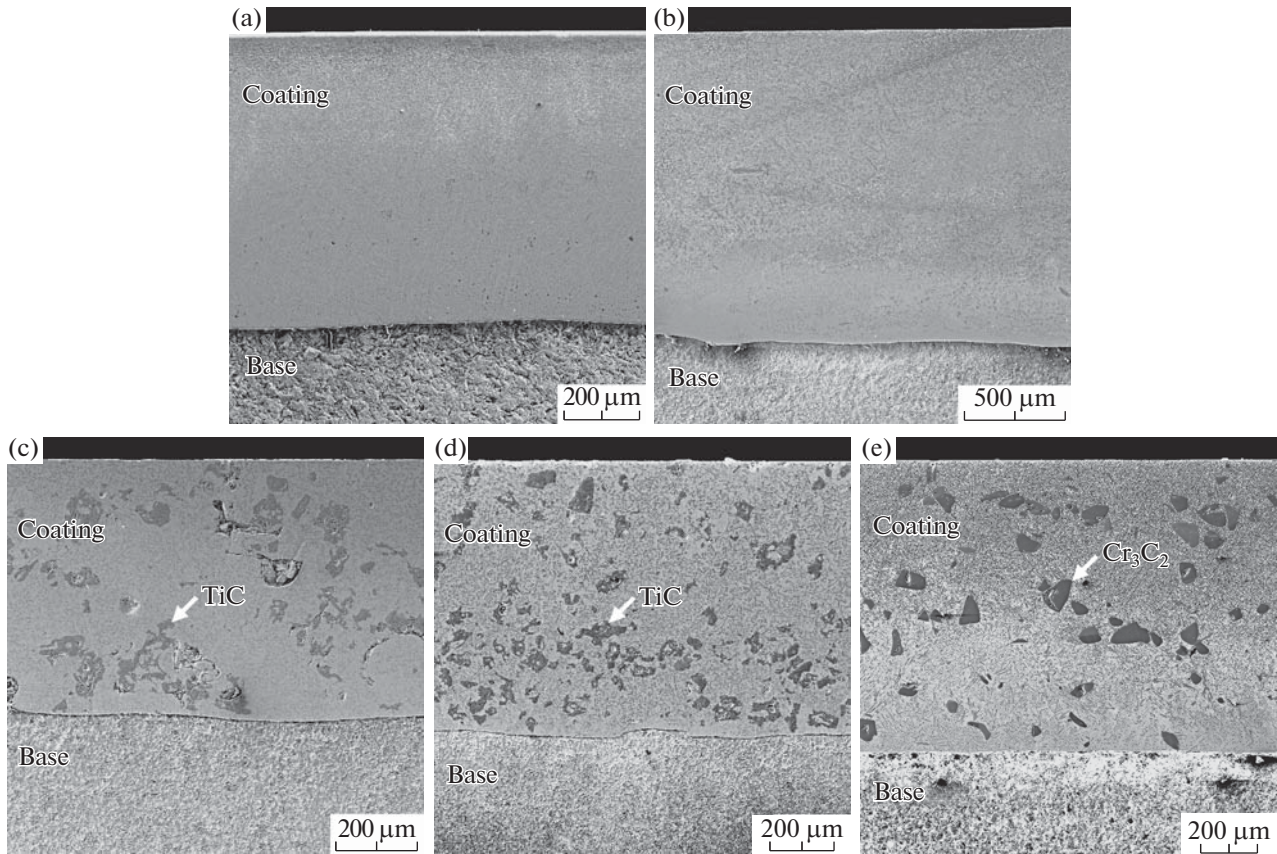


Fig. 2. General appearance of the coatings after laser cladding: (a) PG-SR2, (b) PG-10N-01, and (c–e) PG-SR2 with the additions of (c) 15 wt % TiC, (d) 25 wt % TiC, and (e) 15 wt % Cr_3C_2 .

RESULTS AND DISCUSSION

As a result of the two-layered laser cladding of powder mixtures onto the surface of a plate made of steel St3, chromium–nickel coatings are formed, and this is shown in Fig. 2. The coatings throughout the entire thickness are characterized by a sufficiently uniform distribution of structural components; they have a dendritic structure, in which the direction of dendrites corresponds to that of the temperature gradient during solidification [27]. According to the data of the electron microprobe analysis (EMA), X-ray diffraction analysis [13, 17, 18, 25–27] and to the electron back-scatter diffraction (EBSD) analysis [28], the metallic matrix of the coatings after laser cladding represents a supersaturated Ni-based γ solid solution and a eutectic, which consists of the γ phase and the Ni_3B boride. The formation of the supersaturated solid solutions is characteristic of the processes of laser-induced melting [38]. The strengthening phase in the case of the PG-SR2 coating is the Cr_{23}C_6 carbide. The PG-10N-01 coating, which is alloyed more strongly with carbon, boron, and chromium, contains the carbide Cr_7C_3 and the boride CrB as the strengthening phases. The size of the strengthening phases in the PG-SR2 and PG-10N-01 coatings is in the limits of 1–10 μm .

The composite coatings PG-SR2 also contain the initial coarse (50–150 μm) particles of carbides TiC (see Figs. 2c, 2d) and Cr_3C_2 (see Fig. 2e) that were not dissolved during cladding, and also complex carbides and carboborides. A specific feature of the PG-SR2–TiC composite coatings is the presence in their structure of discontinuities, which are located both inside the coarse particles of TiC and at the boundaries of titanium carbides with the metallic matrix or inside the matrix [17, 18, 26]. In the structure of the composite PG-SR2– Cr_3C_2 coating, we did not observe any such discontinuities [28].

The average microhardness of the PG-SR2 coating is $590 \pm 20 \text{ HV}0.1$. An increase in the content of carbon, boron, and chromium leads to an increase in the average microhardness in the PG-10N-01 coating to values of $970 \pm 40 \text{ HV}0.1$ [25–27]. The addition of particles of titanium carbide in the amounts of 15 and 25 wt % leads to an efficient strengthening of the PG-SR2 coating (to the level 720 ± 40 and $770 \pm 60 \text{ HV}0.1$, respectively) [17, 18, 26]. The composite coating PG-SR2 with the addition of 15 wt % Cr_3C_2 possesses a microhardness of $1080 \pm 110 \text{ HV}0.1$ [28], which substantially exceeds not only the hardness of the base coating, but also the hardness of the compos-

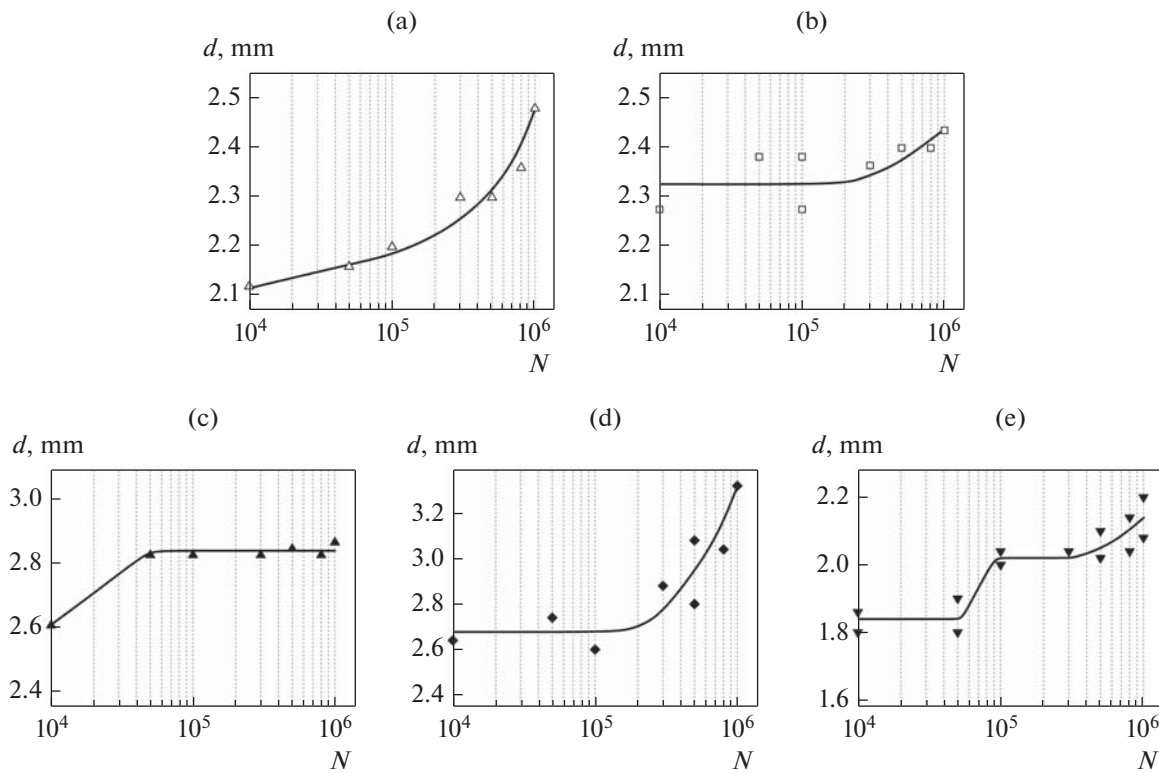


Fig. 3. Effect of the number of cycles of loading N on the diameter of the contact spot d upon the contact fatigue tests of the investigated coatings of (a) PG-SR2, (b) PG-10N-01, and (c–e) PG-SR2 with additions of (c) 15 wt % TiC, (d) 25 wt % TiC, and (e) 15 wt % Cr₃C₂.

ite PG-SR2–TiC coatings with the additions of 15 and 25 wt % titanium carbide.

The results of the contact fatigue tests of the investigated coatings are presented in Fig. 3. As the criterion for the evaluation of the durability of materials under the conditions of the cyclic action of an indenter, we used the changes in the size of the contact spot on the surface of the coating depending on the number of loading cycles [19, 23, 24].

From the data given in Fig. 3, we can see that the diameter of the contact spot after 10^4 loading cycles in the PG-SR2 coating is somewhat more than in the PG-10N-01 coating. This seems to be caused by the higher hardness of the PG-10N-01 coating (970 ± 40 HV0.1) in comparison with the less alloyed PG-SR2 coating (590 ± 20 HV0.1), and by, correspondingly, the increased ability of the PG-10N-01 coating to resist the plastic deformation upon the contact loading. Upon the tests on the base of 10^6 cycles in the PG-SR2 coating we observed a more substantial increase in the size of contact damages than in the PG-10N-01 coating, where there is only an insignificant increase in the diameter of the contact spot (see Figs. 3a, 3b).

The composite coatings PG-SR2 with the addition of TiC, despite their increased levels of microhardness

(720 ± 40 HV0.1 in the coating with the addition 15 wt % of TiC and 770 ± 60 HV0.1 in the coating with the addition of 25 wt % TiC) compared with the initial PG-SR2 coating, are characterized by the largest diameters of the contact spots after 10^4 loading cycles (see Figs. 3c, 3d). This may be caused by the presence of discontinuities in the composite PG-SR2–TiC coatings [17, 18, 26], which, reducing the strength of the material to plastic deformation, lead to an increase in the diameter of the depression upon the cyclic contact loading at the stage of plastic flow (prior to the appearance and development of fatigue cracks). After 3×10^5 loading cycles, in the coating with the addition of 25 wt % TiC we observed a more noticeable increase in the area of the contact spot compared with the coating that contains 15 wt % TiC (see Figs. 3c, 3d). This is likely caused by the presence in the composite coating with the addition of 25 wt % TiC of coarser titanium carbides, which have an embrittling effect, and of a larger quantity of discontinuities than in the coating with 15 wt % TiC [17, 18, 26]. The discontinuities that are present in the composite PG-SR2–TiC coatings also lead to embrittlement because they correspond to locations which are the origin of microscopic cracks. Consequently, an increase in the amount of titanium carbide TiC in the coating from 15 to 25 wt % has a strong embrittling effect and leads to a reduction

Table 2. Results of the microindentation of the samples of investigated coatings at the maximum load on the indenter equal to 1.98 N

Coating	h_{\max} , μm	h_p , μm	HM , GPa	H_{IT} , GPa	E^* , GPa	W_e , μJ	W_t , μJ
PG-SR2	4.02 ± 0.09	3.07 ± 0.34	4.7 ± 0.2	6.3 ± 0.3	195 ± 5	0.68 ± 0.02	2.63 ± 0.07
PG-10N-01	3.43 ± 0.08	2.31 ± 0.18	6.5 ± 0.3	9.7 ± 0.5	193 ± 12	0.81 ± 0.03	2.30 ± 0.10
PG-SR2 +15% TiC	3.99 ± 0.11	2.90 ± 0.25	4.8 ± 0.3	6.9 ± 0.3	161 ± 22	0.81 ± 0.07	2.70 ± 0.08
PG-SR2 +25% TiC	3.76 ± 0.10	2.67 ± 0.99	5.5 ± 0.3	7.6 ± 0.6	197 ± 10	0.72 ± 0.05	2.52 ± 0.09
PG-SR2 +15% Cr_3C_2	3.44 ± 0.05	2.40 ± 0.26	6.4 ± 0.2	9.3 ± 0.3	211 ± 5	0.74 ± 0.01	2.30 ± 0.05

in the contact endurance of the composite coatings, which contain titanium carbides, under the conditions of contact fatigue loading.

In the composite coating PG-SR2 with the addition of Cr_3C_2 , the diameter of the contact spot after 10^4 cycles of loading is smaller (see Fig. 3e) than in the base coating PG-SR2 (see Fig. 3a). This is also caused by the higher hardness of the composite coating PG-SR2–15% Cr_3C_2 compared with the hardness of the base coating PG-SR2, and by, correspondingly, the increased ability of composite coating to resist plastic deformation upon the contact loading. With an increase in the number of cycles of contact loading to 5×10^4 , the diameter of the contact spot of the PG-SR2–15% Cr_3C_2 coating remains almost unchanged. We observed a sharp increase in the diameter of the contact spot at a number of loading cycles of 10^5 . A further loading to 3×10^5 cycles is again accompanied by the stabilization of the diameter of the contact spot, and with an increase in the number of cycles from 5×10^5 to 10^6 we observed a continuous increase in the size of the contact damages (see Fig. 3e); however, this increase is substantially less intensive than in the basic PG-SR2 coating (see Fig. 3a). Consequently, the coarse chromium carbides Cr_3C_2 with a content of 15 wt % do not have an embrittling influence and increase the contact endurance of the composite coating under the conditions of contact fatigue loading.

The presence in the structure of fine dense carbides uniformly distributed in the matrix [39] is assumed to be a favorable condition for increasing the contact fatigue strength of the coatings. However, our results indicate that it is possible to create composite coatings, which contain large particles of the strengthening phases, in particular PG-SR2–15% TiC and PG-SR2–15% Cr_3C_2 , whose contact endurance will not be substantially inferior to the contact endurance of coatings with fine strengthening phases, but other important operating characteristics, for example, wear resistance, can be substantially higher [13, 17, 18].

The size of the contact spot is determined by two basic factors: (1) the plastic deformation (flow of the material) of the surface layer of the coatings under the

action of cyclic contact loading; and (2) the formation of cracks, which weakens the surface layer and leads to an increase in the diameter of the contact spot. Specifically, it is the intensive crack formation [25–28] in the PG-SR2 and PG-SR2–TiC coatings with the addition of 25 wt % TiC upon the specific number of loading cycles (see Figs. 3a, 3d) due to which we observed an accelerated increase in the size of the contact spot in comparison with the PG-10N-01, PG-SR2–TiC coatings with the addition of 15 wt % TiC and PG-SR2– Cr_3C_2 with the addition of 15 wt % Cr_3C_2 (see Figs. 3b, 3c, 3e).

The crack formation develops more actively under the repeated microplastic deformation of the surface layer with cyclic compression [40]. Therefore, both the factors indicated (both plastic deformation and crack formation), which determine the size of the contact spot, and, correspondingly, the durability upon the contact fatigue loading, are caused by the ability of the material to resist plastic deformation upon the cyclic loading. In [27], a new approach was proposed for the evaluation of the ability of materials to withstand the repeated contact loading under the conditions of contact fatigue loading, which is based on the use of a method of microindentation (with a single loading). However, as mentioned above, the contact durability and crack formation of materials with the carbide strengthening depend greatly on the morphology [39] and also on the chemical composition and type of carbides [21]. Therefore, to investigate the possibility of using the method of microindentation (with single loading) for the comparison of the ability of materials with different chemical composition and dispersity of structure to withstand repeated contact loadings under the conditions of contact fatigue loading, we carried out an estimation of the ability of laser-clad surfaces of chromium–nickel coatings to resist mechanical contact action with the use of the data on microindentation.

Table 2 gives the data on the instrumented indentation of the investigated coatings. It can be seen that with an increase in the content of C, Cr, and B, which form the strengthening phases (coating PG-SR2 and PG-10N-01), the values of the maximum and permanent indentation depths h_{\max} and h_p decrease, and the

Table 3. Elastic recovery R_e , ratios H_{IT}/E^* , H_{IT}^3/E^{*2} , and plasticity δ_A of samples made of the coatings investigated

Coating	R_e , %	H_{IT}/E^*	H_{IT}^3/E^{*2} , GPa	δ_A
PG-SR2	23.6	0.032	0.0066	0.74
PG-10N-01	32.7	0.050	0.0245	0.65
PG-SR2 + 15% TiC	27.3	0.043	0.0127	0.70
PG-SR2 + 25% TiC	28.9	0.039	0.0113	0.71
PG-SR2 + 15% Cr ₃ C ₂	30.4	0.044	0.0181	0.68

values of the Martens hardness HM and indentation hardness at the peak load H_{IT} increase. We can also see an increase in the elastic reverse deformation work of the indentation W_e and a reduction in the total mechanical work of the indentation W_t . The modulus of contact elasticity E^* in this case does not change substantially [27].

The data on the results of microindentation of composite coatings are characterized by the fact that with an increase in the Martens hardness HM and the hardness of indentation at the peak load H_{IT} the values of the maximum and permanent indentation depths h_{max} and h_p are reduced in a regular manner. The total mechanical work of the indentation W_t also is reduced because the harder coatings are deformed less during the microindentation. The elastic reverse deformation work of the indentation W_e and the moduli of the contact elasticity E^* of the composite coatings are determined by the specific features of their structure and phase composition and may have various values. We should note the low value of E^* in the composite coating PG-SR2–TiC with 15 wt % TiC (see Table 2), despite the fact that the modulus of elasticity of the titanium carbide TiC is on the order of 440 GPa [41]. We know that the modulus of elasticity of materials is reduced in the presence of porosity [42]. This reduction may therefore be caused by the presence of discontinuities in the structure of the composite coatings PG-SR2–TiC [17, 18, 26]. In the PG-SR2–TiC coating with the addition of 25 wt % TiC the values of E^* are close to those of the base coating PG-SR2 because the influence of porosity is compensated for by the high value of the modulus of elasticity of the titanium carbide TiC, whose content is higher in this coating. In the PG-SR2–Cr₃C₂ coating with the addition of 15 wt % Cr₃C₂, the contact modulus of elasticity is higher than in the base PG-SR2 coating. This is caused by the absence of discontinuities characteristic of the composite PG-SR2–TiC coatings, and by the high value of the modulus of elasticity of the chromium carbide Cr₃C₂, which reaches ~370 GPa [41].

Based on the characteristics measured upon the indentation, we determined parameters which allowed us to estimate the ability of the surface layers of the material to resist mechanical contact action and, correspondingly, to sustain operating loads. Thus, the ratio of the hardness of indentation to the contact modulus of elasticity, H_{IT}/E^* (specific contact hardness) [43, 44], and the elastic recovery $R_e = ((h_{max} - h_p) / h_{max}) \times 100\%$ [45] characterize the elastic deformation (portion of the elastic deformation in the total deformation) and, correspondingly, the ability of material to resist loading without the plastic deformation. The ratio H_{IT}^3/E^{*2} is considered as a qualitative comparative characteristic of the resistance to plastic deformation, since the flow stress is proportional to this ratio ($P_y \sim H^3/E^{*2}$) [46]. These parameters are the characteristics of strength of the material that are determined upon the instrumented indentation. The higher the values of these parameters, the higher the ability of the material to withstand higher contact loads prior to the beginning of plastic deformation and to resist failure upon contact loading.

The plasticity index $\delta_A = 1 - (W_e/W_t)$ characterizes the plasticity of the materials corresponding to the portion of plastic deformation in the total elastic–plastic deformation. The higher the value of this parameter, the higher the plasticity of the material [47].

The data given in Table 3 show that the harder coatings do not always have higher values of the characteristics R_e , H_{IT}/E^* , and H_{IT}^3/E^{*2} determined upon the instrumented microindentation. In particular, the reduction in the value of E^* in the composite coating PG-SR2–TiC containing 15 wt % TiC, which is caused by the presence of discontinuities in its structure [17, 18, 26], ensures higher values of H_{IT}^3/E^{*2} than in the harder coating PG-SR2–TiC with the addition of 25 wt % TiC (see Table 2).

We can see from Fig. 4 that there is a correlation dependence between the diameter of the contact spot

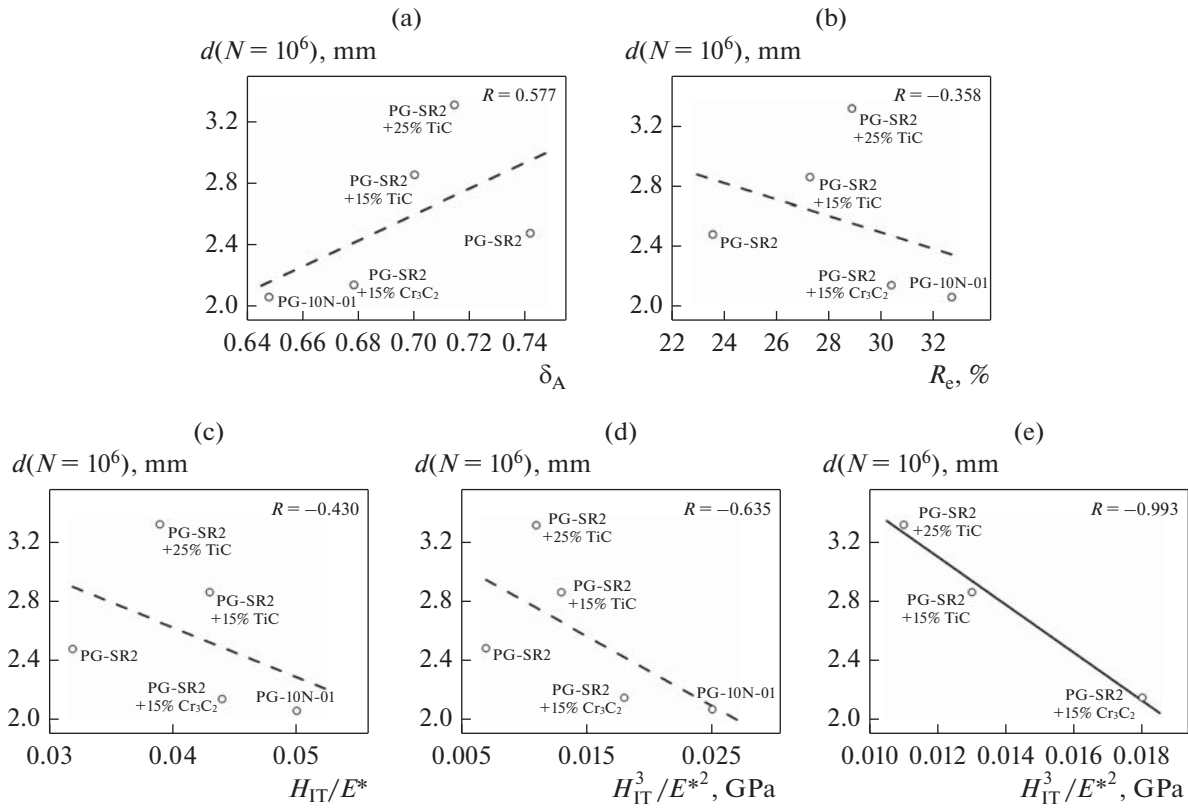


Fig. 4. Relationship between the diameter of the contact spot $d(N = 10^6)$ upon the contact fatigue tests after $N = 10^6$ loading cycles and (a) the plasticity δ_A , (b) elastic recovery R_e , (c) specific contact hardness H_{IT}/E^* , and (d, e) the ratio of the exponentials H_{IT}^3/E^{*2} of the investigated coatings; R is the correlation coefficient.

upon the contact fatigue tests after $N = 10^6$ loading cycles $d(N = 10^6)$ on the one hand, and the plasticity δ_A , the elastic recovery R_e , the specific contact hardness H_{IT}/E^* , and the power ratio H_{IT}^3/E^{*2} on the other hand. It can be seen that in the case of the simultaneous analysis of coatings with different dispersities of the strengthening phases, the correlation coefficients are low. However, we observed a strong linear correlation between the diameter of the contact spot $d(N = 10^6)$ and the power ratio H_{IT}^3/E^{*2} for the subgroup of coatings with coarse strengthening phases (see Fig. 4e), which can be described by the following equation (R is the correlation coefficient):

$$d(N = 10^6) = -163.85 H_{IT}^3/E^{*2} + 5.07, \\ R = -0.993.$$

For the subgroup of coatings with fine strengthening phases, we could expect to see a correlation between the diameter of the contact spot in the contact fatigue tests and the parameters determined upon the instrumented indentation. However, the number of experimental points has until now been insufficient to make a single-valued conclusion about the presence

of this correlation. We will investigate this in further experiments.

CONCLUSIONS

We studied the contact endurance of laser-clad chromium–nickel coatings of the NiCrBSi system with different contents of chromium, boron, carbon, and additions of titanium carbide TiC (15 and 25 wt %) and chromium carbide Cr_3C_2 (15 wt %) upon contact fatigue loading according to the scheme of the pulsing non-impact “sphere-to-surface” contact. We established that the contact endurance of chromium–nickel coatings with different chemical composition and different dispersity of the structure is determined by their ability to resist plastic deformation under the conditions of the repeated elastic–plastic deformation upon the mechanical non-impact contact action. The basic mechanisms of the formation of the contact spot in this case are plastic deformation and crack formation. We have shown that it is possible to create composite coatings containing large (50–150 μm) particles of the strengthening phases, in particular, PG-SR2–15% TiC and PG-SR2–15% Cr_3C_2 , whose contact endurance would not be greatly inferior to the contact

endurance of coatings with fine (1–10 μm) strengthening phases.

We estimated the ability of the surface of chromium–nickel coatings to resist mechanical contact action based on microindentation data. It became clear that there is a strong linear correlation between the diameter of the contact spot $d(N = 10^6)$ and the power ratio H_{IT}^3/E^{*2} for the subgroup of coatings with coarse strengthening phases. We have therefore shown that the method of microindentation (single loading) can be used to determine the ability of chromium–nickel coatings to withstand repeated contact loadings.

ACKNOWLEDGMENTS

The work was performed within the framework of the state task for the Institute of Engineering Science, Ural Branch, Russian Academy of Sciences, according to the theme no. AAAA-A18-118020790147-4. The scanning electron microscopy and the mechanical and micromechanical tests were performed at the Center of the Collaborative Access “Plastometriya” of the Institute of Engineering Science, Ural Branch, Russian Academy of Sciences. The author is grateful to the Doct. of Eng. Sci. A.V. Makarov for participation in the discussion of results, to Cand. of Eng. Sci. I.Yu. Malygina and to Cand. of Eng. Sci. N.N. Soboleva for their assistance in conducting these studies, and to Cand. of Eng. Sci. A.L. Osintseva for the application of coatings by the method of laser cladding.

REFERENCES

1. A. G. Grigor'yants and A. N. Safonov, *Laser Techniques and Technology. In 7 books. Book. 3. Methods of Surface Laser Treatment* (Vysshaya Shkola, Moscow, 1987) [in Russian].
2. C. Navas, R. Colaço, J. de Damborenea, and R. Vilar, “Abrasive wear behavior of laser clad and flame sprayed-melted NiCrBSi coatings,” *Surf. Coat. Technol.* **200**, 6854–6862 (2006).
3. E. Fernández, M. Cadenas, R. González, C. Navas, R. Fernández, and J. de Damborenea, “Wear behaviour of laser clad NiCrBSi coating,” *Wear* **259**, 870–875 (2005).
4. A. V. Makarov and N. N. Soboleva, “Formation of wear-resistant NiCrBSi coatings by laser surfacing and combined treatments.” in *Promising Materials. Vol. VII: A Textbook*, Ed. by D. L. Merson (TGU, Tolyatti, 2017) [in Russian], ch. 5, pp. 167–238.
5. C. Katsich and E. Badisch, “Effect of carbide degradation in a Ni-based hardfacing under abrasive and combined impact/abrasive conditions,” *Surf. Coat. Technol.* **206**, 1062–1068 (2011).
6. K. Gurumoorthy, M. Kamaraj, K. Rao Prasad, A. Rao Sambasiva, and S. Venugopal, “Microstructural aspects of plasma transferred arc surfaced Ni-based hardfacing alloy,” *Mater. Sci. Eng., A* **456**, 11–19 (2007).
7. B. Cai, Y.-f. Tan, He L., Tan H., and Gao L., “Tribological properties of TiC particles reinforced Ni-based alloy composite coatings,” *Trans. Nonferrous Met. Soc. China* **23**, 1681–1688 (2013).
8. A. V. Makarov, N. N. Soboleva, I. Yu. Malygina, and A. L. Osintseva, “Formation of wear-resistant chromium–nickel coating with extra high thermal stability by combined laser-and-heat treatment,” *Met. Sci. Heat Treat.* **57**, 161–168 (2015).
9. T. Liyanage, G. Fisher, and A. P. Gerlich, “Influence of alloy chemistry on microstructure and properties in NiCrBSi overlay coatings deposited by plasma transferred arc welding (PTAW),” *Surf. Coat. Technol.* **205**, 759–765 (2010).
10. A. V. Makarov, R. A. Savrai, A. L. Osintseva, and I. Yu. Malygina, “The influence of the chemical composition on the tribological properties of chromium–nickel coatings obtained by the method of gas-powder laser cladding,” *Izv. Chelyabinsk NTs UrO RAN*, No. 2 (44), 28–33 (2009).
11. A. V. Makarov, E. S. Gorkunov, I. Yu. Malygina, L. Kh. Kogan, R. A. Savrai, and A. L. Osintseva, “Eddy-current testing of the hardness, wear resistance, and thickness of coatings prepared by gas-powder laser cladding,” *Russ. J. Nondestr. Test.* **45**, 797–805 (2009).
12. N. N. Soboleva, I. Yu. Malygina, A. L. Osintseva, and N. A. Pozdeeva, “The influence of the microstructure and phase composition on tribological performances of NiCrBSi laser coatings,” *Izvestia of RAS SamSC* **13**, 869–873 (2011).
13. A. V. Makarov, N. N. Soboleva, and I. Yu. Malygina, “Role of the strengthening phases in abrasive wear resistance of laser-clad NiCrBSi coatings,” *J. Frict. Wear* **38**, 272–278 (2017).
14. A. Zikin, E. Badisch, I. Hussainova, C. Tomastik, and H. Danning, “Characterisation of TiC–NiMo reinforced Ni-based hardfacing,” *Surf. Coat. Technol.* **236**, 36–44 (2013).
15. X. H. Wang, M. Zhang, X. M. Liu, S. Y. Qu, and Z. D. Zou, “Microstructure and wear properties of TiC/FeCrBSi surface composite coating prepared by laser cladding,” *Surf. Coat. Technol.* **202**, 3600–3606 (2008).
16. S. Yang, W. Liu, M. Zhong, and Z. Wang, “TiC reinforced composite coating produced by powder feeding laser cladding,” *Mater. Lett.* **58**, 2958–2962 (2004).
17. A. V. Makarov, N. N. Soboleva, I. Yu. Malygina, and A. L. Osintseva, “The formation of NiCrBSi–TiC composite coating with increased abrasive wear resistance by gas powder laser cladding,” *Uprochn. Tekhnol. Pokr.*, No. 11 (107), 38–44 (2013).
18. A. V. Makarov, N. N. Soboleva, I. Yu. Malygina, and A. L. Osintseva, “The tribological performances of a NiCrBSi–TiC laser-clad composite coating under abrasion and sliding friction [Digital resource],” *Diagn. Resour. Mech. Mater. Struct.*, No. 3, 83–97 (2015). http://dream-journal.org/Issues/2015-3/2015-3_33.html.
19. L. I. Tushinskii, V. A. Bataev, V. M. Potapov, A. A. Bataev, and A. P. Timofeev, “Life of hardened materials under the conditions of contact load,” *Met. Sci. Heat Treat.* **30**, 363–365 (1988).

20. A. Yonezu, B. Xu, and X. Chen, “An experimental methodology for characterizing fracture of hard thin films under cyclic contact loading,” *Thin Solid Films* **518**, 2082–2089 (2010).
21. G. Ramírez, A. Mestra, B. Casas, I. Valls, R. Martínez, R. Bueno, A. Goetz, A. Mateo, and L. Llanes, “Influence of substrate microstructure on the contact fatigue strength of coated cold-work tool steels,” *Surf. Coat. Technol.* **206**, 3069–3081 (2012).
22. G. Ramírez, E. Tarrés, B. Casas, I. Valls, R. Martínez, and L. Llanes, “Contact fatigue behavior of PVD-coated steel,” *Plasma Processes Polym.* **6**, S588–S591 (2009).
23. E. Tarrés, G. Ramírez, Y. Gaillard, E. Jiménez-Piqué, and L. Llanes, “Contact fatigue behavior of PVD-coated hardmetals,” *Int. J. Refract. Met. Hard Mater.* **27**, 323–331 (2009).
24. I. A. Bataev, A. A. Bataev, M. G. Golkovski, D. S. Krivizhenko, A. A. Losinskaya, and O. G. Lenivtseva, “Structure of surface layers produced by non-vacuum electron beam boriding,” *Appl. Surf. Sci.* **284**, 472–481 (2013).
25. R. A. Savrai, A. V. Makarov, N. N. Soboleva, I. Yu. Malygina, and A. L. Osintseva, “The contact endurance of NiCrBSi coatings obtained by gas powder laser cladding,” *Obrab. Met.*, No. 4 (65), 43–51 (2014).
26. R. A. Savrai, A. V. Makarov, E. S. Gorkunov, L. Kh. Kogan, N. N. Soboleva, I. Yu. Malygina, and A. L. Osintseva, “Eddy-current testing of fatigue degradation under contact loading of NiCrBSi coatings obtained through gas–powder laser cladding,” *Russ. J. Nondestr. Test.* **51**, 692–704 (2015).
27. R. A. Savrai, A. V. Makarov, N. N. Soboleva, I. Yu. Malygina, and A. L. Osintseva, “The behavior of gas powder laser clad NiCrBSi coatings under contact loading,” *J. Mater. Eng. Perform.* **25**, 1068–1075 (2016).
28. R. A. Savrai, A. V. Makarov, E. S. Gorkunov, N. N. Soboleva, L. Kh. Kogan, I. Yu. Malygina, A. L. Osintseva, and N. A. Davydova, “Eddy-current testing of the fatigue degradation of a gas powder laser clad NiCrBSi–Cr₃C₂ composite coating under contact fatigue loading,” *AIP Conf. Proc.* **1915**, No. 040049, 1–4 (2017).
29. H.-F. Xuan, Q.-Y. Wang, S.-L. Bai, Z.-D. Liu, H.-G. Sun, and P.-Ch. Yan, “A study on microstructure and flame erosion mechanism of a graded Ni–Cr–B–Si coating prepared by laser cladding,” *Surf. Coat. Technol.* **244**, 203–209 (2014).
30. Š. Houdková, E. Smazalová, M. Vostřák, and J. Schubert, “Properties of NiCrBSi coating, as sprayed and remelted by different technologies,” *Surf. Coat. Technol.* **253**, 14–26 (2014).
31. A. V. Makarov, N. A. Pozdejeva, R. A. Savrai, A. S. Yurovskikh, and I. Yu. Malygina, “Improvement of wear resistance of quenched structural steel by nanostructuring frictional treatment,” *J. Friction Wear* **33**, 433–442 (2012).
32. V. P. Kuznetsov, A. V. Makarov, S. G. Psakhie, R. A. Savrai, I. Yu. Malygina, and N. A. Davydova, “Tribological aspects in nanostructuring burnishing of structural steels,” *Phys. Mesomech.* **17**, 250–264 (2014).
33. A. V. Makarov, N. N. Soboleva, R. A. Savrai, and I. Yu. Malygina, “Improving the micromechanical properties and wear resistance of nickel-chromium laser clad coating using finishing frictional treatment,” *Vektor Nauki TGU*, No. 4 (34), 60–67 (2015).
34. N. B. Pugacheva, E. B. Trushina, and T. M. Bykova, “Research on the tribological properties of iron borides as diffusion coatings,” *J. Friction Wear* **35**, 489–496 (2014).
35. N. B. Pugacheva, T. M. Bykova, and E. B. Trushina, “The steel-basis structure influence on the diffusion boride coatings structure and properties,” *Uprochn. Tekhnol. Pokr.*, No. 4 (100), 3–7 (2013).
36. R. A. Savrai and A. V. Makarov, RF Patent No. 162959, *Byull. Izobret.*, No. 19 (2016).
37. GOST R 8.748-2011 (ISO 14577-1:2002) State system for ensuring the uniformity of measurements (ICG). Metals and alloys. Measurement of hardness and other characteristics of materials in tool indenting. Part 1. Testing method.
38. E. V. Kharanzhevskiy, “Separation in liquid and the formation of supersaturated solid solutions in Fe–Cu alloys upon rapid laser melting,” *Phys. Met. Metallogr.* **117**, 889–895 (2016).
39. L. Llanes, E. Tarrés, G. Ramírez, C. A. Botero, and E. Jiménez-Piqué, “Fatigue susceptibility under contact loading of hardmetals coated with ceramic films,” *Procedia Eng.* **2**, 299–308 (2010).
40. A. I. Popelyukh, P. A. Popelyukh, A. A. Bataev, A. A. Nikulina, and A. I. Smirnov, “Specific features of the nucleation and growth of fatigue cracks in steel under cyclic dynamic compression,” *Phys. Met. Metallogr.* **117**, 279–287 (2016).
41. *CRC Materials Science and Engineering Handbook, Third Edition*, Ed. by W. Alexander and J. F. Shackelford (CRC Press, Boca Raton, 2000).
42. J. Kováčik, “Correlation between Young’s modulus and porosity in porous materials,” *J. Mater. Sci. Lett.* **18**, 1007–1010 (1999).
43. Y. T. Cheng and C. M. Cheng, “Relationships between hardness, elastic modulus and the work of indentation,” *Appl. Phys. Lett.* **73**, 614–618 (1998).
44. S. A. Firstov, V. F. Gorban’, and E. P. Pechkovskii, “Measurement of ultimate values of hardness, elastic strain and stress of materials by an automatic indentation method,” *Materialovedenie*, No. **8**, 15–21 (2008).
45. T. F. Page and S. V. Hainsworth, “Using nanoindentation techniques for the characterization of coated systems: A critique,” *Surf. Coat. Technol.* **61**, 201–208 (1993).
46. P. H. Mayrhofer, C. Mitterer, and J. Musil, “Structure–property relationships in single- and dual-phase nanocrystalline hard coatings,” *Surf. Coat. Technol.* **174–175**, 725–731 (2003).
47. Yu. V. Milman, S. I. Chugunova, and I. V. Goncharova, “Plasticity characteristic obtained by indentation,” *Vopr. At. Nauki Tekh.*, No. 4, 182–187 (2011).

Translated by S. Gorin